



Science Arts & Métiers (SAM)

is an open access repository that collects the work of Arts et Métiers Institute of Technology researchers and makes it freely available over the web where possible.

This is an author-deposited version published in: <https://sam.ensam.eu>
Handle ID: <http://hdl.handle.net/10985/9634>

To cite this version :

Isabelle DERUE, Pierre GILORMINI, Jacques VERDU, Cyril VAULOT, Marie COQUILLAT, Nancy DESGARDIN, Aude VANDENBROUKE, Emmanuel RICHAUD - Platicizer effect on network structure and hydrolytic degradation - European Polymer Journal - Vol. 60, p.232-246 - 2015

Any correspondence concerning this service should be sent to the repository

Administrator : scienceouverte@ensam.eu



PLASTICIZER EFFECT ON NETWORK STRUCTURE AND HYDROLYTIC DEGRADATION

By Emmanuel Richaud^{1*}, Isabelle Derue¹, Pierre Gilormini¹, Jacques Verdu¹, Cyril Vaultot², Marie Coquillat³, Nancy Desgardin³, Aude Vandenbrouke³

1. Laboratoire Procédés et Ingénierie en Mécanique et Matériaux (PIMM), ENSAM, CNRS, CNAM, 151 boulevard de l'Hôpital, 75013 Paris, France.

2. Institut de Science des Matériaux de Mulhouse (IS2M), CNRS, 15 Rue Jean Starcky, 68057 Mulhouse Cedex, France.

3. Herakles Groupe Safran, Direction Technique, Centre de Recherches du Bouchet, 9, rue Lavoisier, 91710 Vert le Petit, France.

* Corresponding author : emmanuel.richaud@ensam.eu

ABSTRACT

The hydrolytic degradation of fully cured polyester-urethane networks polymerized in the presence of several weight ratios of triacetin was monitored by the residual concentration in elastically active chains obtained from modulus and equilibrium solvent swelling measurements. The presence of triacetin does not change the water uptake but induces a lower rate of degradation. Comparisons were performed with networks in which triacetin was removed before ageing, and with networks in which polyester-urethane was first polymerized and then impregnated by triacetin. Data suggest that the presence of triacetin during polymerization induces the presence of elastically inactive chains such as dangling chains, loops... the hydrolysis of which does not change the elastic properties of the network. This explanation was checked from relaxation measurements by n.m.r and d.m.a, and by the analysis of the soluble fraction generated by hydrolysis.

KEYWORDS

Hydrolysis, polyester-urethane, rubber elasticity, plasticizer

INTRODUCTION

Water induces degradation of polyester-based polymers. Their mechanical properties can be altered by essentially two ways: the plasticization induced by water penetration in the initially glassy network [1,2], or the chemical reaction between cleavable ester groups and water [2,3,4]. Both processes can take place together or separately. In the first case, an equilibrium state can be reached, whereas the second process is expected to lead to a continuous decrease of the network mechanical properties till a “degelation” point is reached. At this point, all elastically active chains are cut, the polymer becomes fully soluble, and it turns back to a liquid polymer.

There is a well-documented literature dealing with several aspects of polymer hydrolysis:

- structure-properties relationships highlighting the effect of structure on hydrophilicity [5,6], but there is much less work dealing with the relationship between macromolecular architecture and the sensitivity to chain scission.
- kinetic modeling of direct, reversible and diffusion controlled hydrolysis [7,8].
- modeling of elastically active chains consumption exploring for example the influence of the average number of cleavable bonds hold by elastically active chains on the degelation process [9].

This literature is based on “model” systems: linear thermoplastic polymers, ideal networks (i.e., networks in which all chains are elastically active), polymers with only one kind of reactive units. Less is known about the cases where:

- the polymer is compounded with additives such as plasticizers. The influence of plasticizers on rheological and initial mechanical properties is well documented [10,11,12,13]. Some studies already dealt with the influence of additives on physical ageing through the permeability of water into polymers [14,15], but additives can also participate in the hydrolytic process through catalytic effects as suggested by a recent work [16].

- the polymer contains “structural defects” (i.e., is non-ideal), since the architecture of the final gel and the possibility of cyclization strongly depend on the presence of a solvent that would “swell” the polymer during its crosslinking [17], even if this issue was ignored for an elastomer cured in the presence of a plasticizer content up to 40% [12].

Therefore, this paper investigates the hydrolytic degradation of polyester-urethane networks containing up to 75% weight ratios of triacetin, which is an inert plasticizer that does not participate “actively” to the crosslinking process [18,19]. Special attention will be paid to the effects of triacetin on:

- Water permeation.

- Network architecture. As a matter of fact, a plasticizer acts as a diluent in the polymerization medium and, consequently, is expected to change the network architecture and possibly its sensitivity towards hydrolysis. This is the reason why samples polymerized in the presence of triacetin will be compared with other samples polymerized without diluent but with the plasticizer added after polymerization.

EXPERIMENTAL

1. Materials

1.1. Networks synthesized in the presence of triacetin

The polyester under study is a polycondensate resulting from the reaction of 60% by weight adipic acid, 12% ethylene glycol and 28% diethylene glycol. Its number average molar mass is c.a. 2100 g mol⁻¹ and its polydispersity index is close to 1.7. This macrodiol was crosslinked 14 days at 50°C by a stoichiometric amount of benzene triisocyanate in molds to produce foils of 2 mm thickness. Dogbone H3 samples of calibrated length (20 mm) and width (4 mm) were cut from these foils.

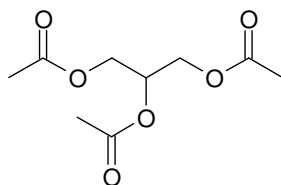


Figure 1. Structure of triacetin.

In the present case, the polyester-urethane networks were synthesized in the presence of triacetin used as a plasticizer. The weight ratios of triacetin under investigation were 0, 0.25, 0.5 and 0.75. They will be considered equal to volume ratios since the density of polyester-urethane and triacetin are respectively close to 1.2 and 1.16. These materials will be denoted as P, P+TA 75/25, P+TA 50/50 and P+TA 25/75 in the following.

1.2. Networks containing a plasticizer added after synthesis

Measurements of triacetin sorption by polyester-urethane P (polymerized in undiluted state and expected to be ideal networks – see “RESULTS” section) were performed at 23°C, 60°C and 80°C (Figure 2). The triacetin equilibrium mass uptake was almost constant (about 130 ± 10 %) in the whole temperature range under study and corresponded to a triacetin weight fraction of about 56 ± 2 %. For example, the triacetin content in a sample impregnated during ca 16h or 70 h at room temperature was ca 25 or 50% in weight. These materials are denoted as P+TA 75/25_{impregnated} and P+TA 50/50_{impregnated}.

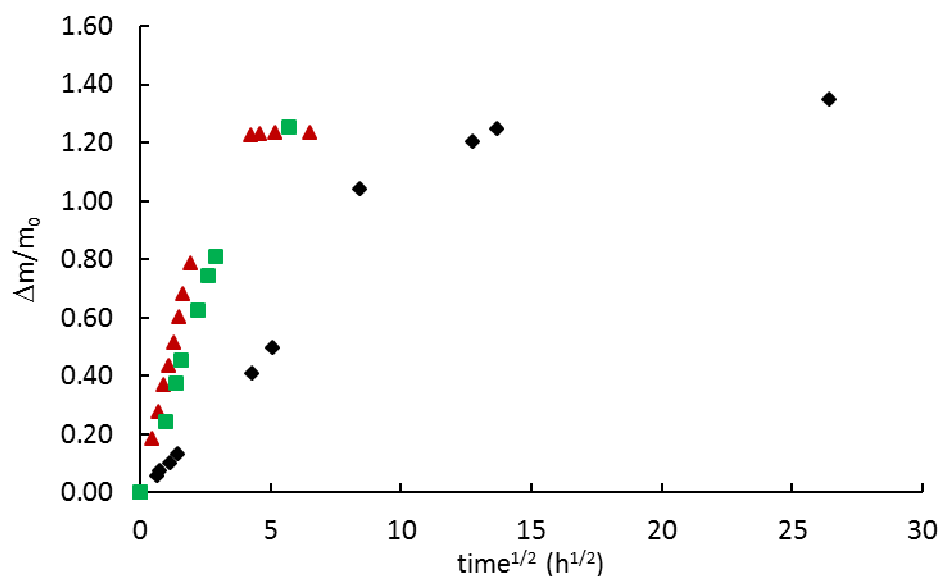


Figure 2. Kinetics of triacetin mass uptake into polyester-urethane P at 23 (◆), 60 (■), and 80°C (▲).

NB: square root of time is chosen as abscissa axis for better clarity.

1.3. Networks in which the plasticizer added during synthesis is removed before ageing

Some comparisons were done with networks polymerized in the presence of triacetin and in which the latter was totally extracted by 1,2-dichloroethane (72 h at room temperature). These materials are denoted P+TA 50/50_{extracted} and P+TA 25/75_{extracted} in the following.

2. Ageing tests

The samples were submitted to humid ageing at 60°C under 29 and 75% relative humidity obtained from saturated solutions of MgCl₂·6H₂O and NaCl, respectively. Relative humidity and temperature were checked regularly using a MicroLog PRO II Humidity Data Logger (Fourtec Technology).

3. Characterization

3.1. Water permeation by dynamic vapor sorption (DVS)

The polymer affinity with water was measured by keeping ca. 20 mg samples in air at 1 bar with fixed water partial pressures between 0 and 90% in a dynamic vapor sorption apparatus DVS-1000 from Surface Measurement Systems. DVS measurements were also used for comparing the affinity of each sort of polyester-urethane with 1,2-dichloroethane used as a solvent for sol-gel analysis.

3.2. Modulus measurement by mechanical tests

Uniaxial tension was performed at 20°C and at 10 mm min⁻¹ (8.33×10⁻³ s⁻¹) strain rate, using an INSTRON 4301 machine with a 100 N cell. The engineering stress F/S_0 was recorded against $(\lambda - \lambda^{-2})$, where λ denotes the draw ratio, so that the initial slope of the curve is the shear modulus G from which the concentration in elastically active chains is deduced [20].

3.3. Sol gel analysis

Virgin or aged samples were characterized by monitoring their equilibrium swelling ratio in 1,2-dichloroethane (ACS reagent, Carlo Erba). Data were exploited for quantifying:

1) the soluble fraction $SF = (m_0 - m_{dry})/m_0$,

2) the equilibrium swell ratio $SW = m_{swollen}/m_{dry}$ from which the polymer volume ratio in swollen network (denoted by ϕ_2) can be calculated:

$$\phi_2 = \left[1 + \frac{\rho_2}{\rho_1} \cdot (SW - 1) \right]^{-1} \quad (1)$$

where ρ_1 and ρ_2 denote the 1,2-dichloroethane density and the polymer density, respectively. The elastically active chain concentration in the dry polymer ([EAC]) is then calculated using the Flory-Rehner theory [20]:

$$[\text{EAC}] = - \frac{\ln(1-\phi_2) + \phi_2 + \chi_{12}\phi_2^2}{V_{1m} \cdot \left(\phi_2^{1/3} - \frac{2}{f} \cdot \phi_2 \right)} \quad (2)$$

where V_{1m} is the solvent molar volume, f is the crosslink functionality (taken equal to 3), χ_{12} is the polymer-1,2-dichloroethane interaction parameter taken equal to 0.3 from DVS measurements at room temperature. It was checked that χ_{12} was very close for all the materials under study.

3.4. Low field nuclear magnetic resonance (NMR)

The low field NMR apparatus (20 MHz) is supplied by Bruker under the commercial name of Minispec®. The measurement temperature was regulated with ± 0.1 K accuracy and manually checked with a thermocouple. Different NMR relaxation sequences were used to determine the structure and the organization of the materials by studying the various mobility modes:

1) T_1 by inversion-recovery (180° - τ - 90°) [21,22].

2) T_2 by spin (Hahn) echo (90° - τ - 180° - τ -echo) [23] and by solid echo [21]. The solid echo studies were realized with $\tau = 0.0095$ ms. The Hahn echo studies were realized first at one echo time ($\tau = 0.0095$ ms) and then with a varying echo between $\tau = 0.0095$ ms and $\tau = 10$ ms.

3) T_2 by the Carr-Purcell-Meiboom-Gill (CPMG) method ($90^\circ_x(-\tau-180^\circ_y-\tau\text{-echo})_n$) [20,21]. The echo time was $\tau = 0.05$ ms.

3.5. Dynamical mechanical analysis (DMA)

The samples were characterized by dynamic mechanical analysis using a DMA Q800 apparatus (TA Instruments) driven by Q Series Explorer. The samples were submitted to:

- 1) Temperature sweep tests performed at $2^{\circ}\text{C min}^{-1}$ heating ramp, at 1 Hz frequency in tension mode, at a 0.1% strain with a 0.5 N preload force.
- 2) Frequency sweep tests at several temperatures in tension mode at a 0.1% strain with a 0.5 N preload force.
- 2) Relaxation tests at -30°C under 5 % strain with a 0.001 N preload force.

3.6. Fourier transform infrared spectroscopy (FTIR)

The hydrolytic stability of triacetin was also investigated by the analysis of virgin or aged triacetin directly dropped on the ATR crystal of the FTIR apparatus. The analysis consisted in the average of 32 scans at a 4 cm^{-1} resolution.

RESULTS

1. Initial characterization of networks

1.1. Water permeation

The water uptake was recorded and the resulting sorption isotherms at 60°C are presented in Figure 3 for polyester-urethane P and P+TA 50/50. The presence of triacetin appears not to change significantly the water uptake in polyester-urethane whatever the relative humidity. This is consistent with the above observation on 1-2 dichloroethane absorption.

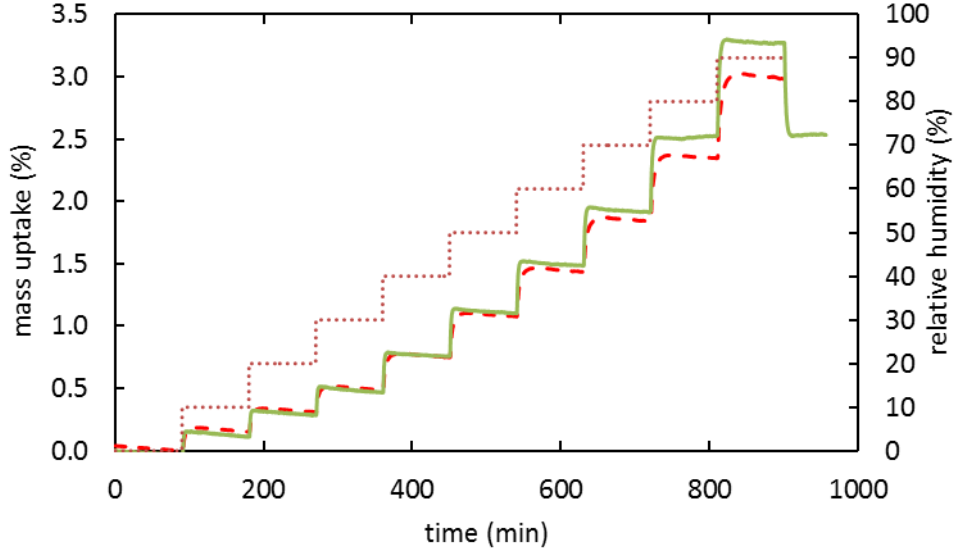


Figure 3. Water uptake measurements recorded by DVS at 60°C at several partial water pressures (...) for polyester-urethane P (---) and P+TA 50/50 (—).

1.2. Concentration in elastically active chains

Figure 4 shows the tensile stress-strain curves for the polyester-urethanes polymerized in the presence of triacetin. The curves were replotted as nominal stress vs. $(\lambda - \lambda^{-2})$, λ being the stretch ratio. These plots are linear and their slopes give the concentrations in elastically active chains by [24]:

$$\frac{F}{S_0} = [\text{EAC}] \cdot \phi_p^{1/3} \cdot RT \cdot (\lambda - \lambda^{-2}) \quad (3)$$

With:

$$[\text{EAC}] = \frac{\rho_2}{M_c} \quad (4)$$

where ϕ_p is the polymer volume fraction in the polyester-urethane plus triacetin mixture, and M_c is the molar mass between crosslink nodes.

The resulting concentrations in elastically active chains (Table 1) can be commented as follows:

1) For the pure polyester-urethane network, $M_c = \rho/[EAC]$ is close to the average molar mass of prepolymer (2.1 kg mol^{-1}), which suggests this network is very close to ideality, i.e., all the polyester chains are elastically active.

2) $[EAC]$ decreases continuously when the triacetin/polymer ratio increases. Since $[EAC]$ is corrected here to take into account the diluting effect of triacetin (through the $\phi_p^{1/3}$ term in Eq. 3), the observed decrease of $[EAC]$ suggests that P+TA 75/25, and more specially P+TA 50/50 and P+TA 25/75, have a macromolecular architecture that differs from the pure polyester-urethane network.

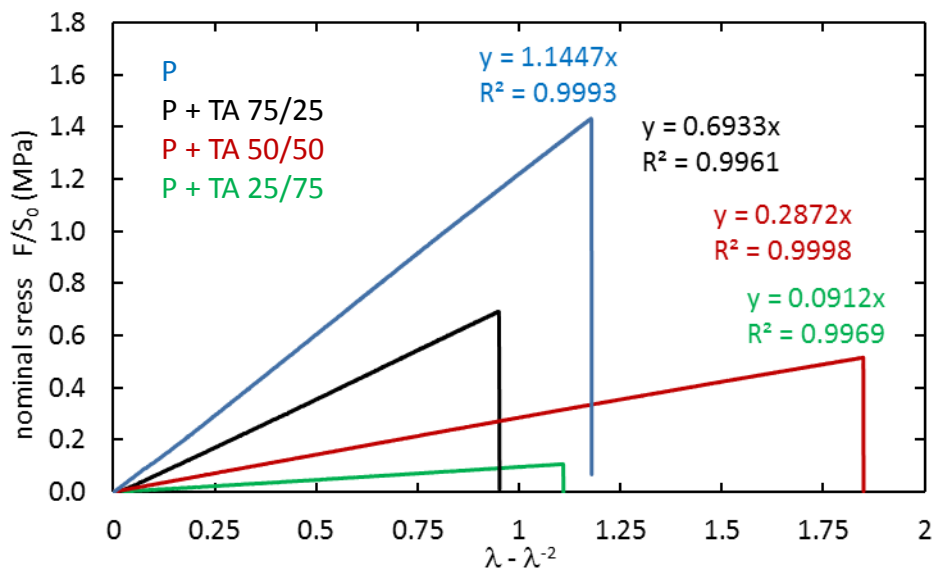


Figure 4. Stress strain curves for polyester-urethanes polymerized in the presence of triacetin.

The networks were also characterized by 1-2 dichloroethane sorption using DVS measurements. The initial slopes of the sorption isotherms, which determine the interaction parameter value χ_{12} [20], were found almost independent of the triacetin weight fraction. This is not surprising, since the unique dipolar contribution to cohesive energy is due to the ester groups in the polymer and in

triacetin. Using the same interaction parameter value $\chi_{12} = 0.3$ for all the samples under study, the [EAC] estimations from mechanical tests and from equilibrium swelling using the above equations are in good agreement (Table 1) and they will be used without distinction in the following.

		P	P+TA (75/25)	P+TA (50/50)	P+TA (25/75)	P + TA 50/50 _{extracted}	P + TA 25/75 _{extracted}
tensile test	$\sigma_{nom}/(\lambda-\lambda^{-2})$ (MPa)	1.206	0.768	0.306	0.107		
	EAC (mol l ⁻¹)	0.487	0.341	0.156	0.068		
sol gel	Swelling Ratio	4.191	4.462	7.283	10.252		
	EAC (mol l ⁻¹)	0.454	0.393	0.118	0.069		
DMTA	E' _{glassy} (MPa)	720		2010	2450	1200	1650
	E' _{rubbery} (MPa)	3.63		0.91	0.18	1.36	0.5
	Tg (°C)	-28		-43.8	-54.9	-30.1	-34.9
	(tan delta) _{max}	1.66		2.88	5.54	1.86	1.81

Table 1. Initial characterization of the polyester-urethane networks (see Figures 4 and 5).

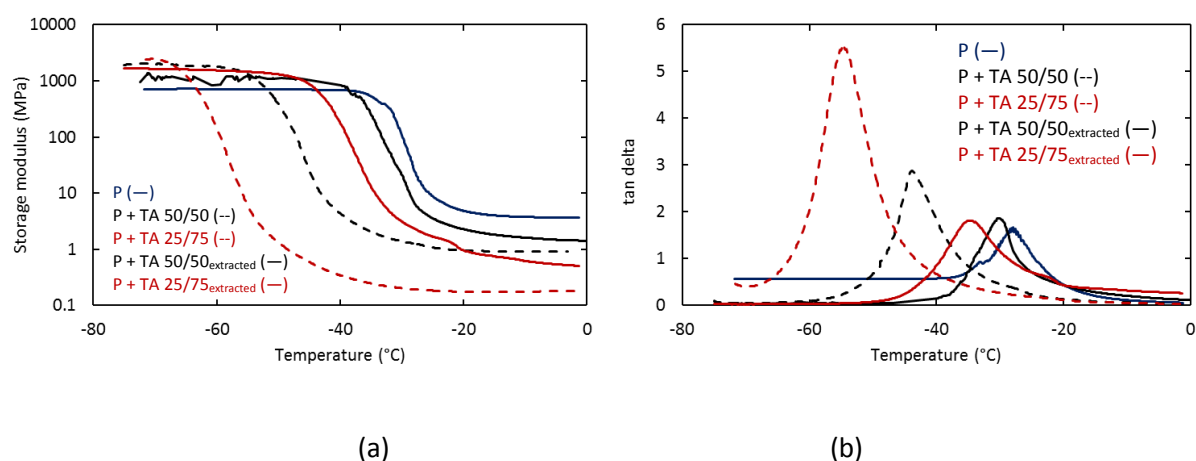


Figure 5. Storage modulus E' (a) and loss factor (b) versus temperature.

Figure 5 shows the results of a temperature sweep monitored by DMA for pure polyester-urethane, polyester-urethane with 50 and 75% of triacetin, and for these two materials after triacetin removal. These results call for the following comments:

1) DMTA and tensile testing lead to consistent results since E' measured from DMTA is expected to be equal to $3.G$ where $G = \sigma_{nom}/(\lambda-\lambda^{-2})$ measured from tensile testing.

2) The comparison of the “swollen” samples P+TA 50/50 and P+TA 25/75 with the corresponding extracted samples P+TA 50/50_{extracted} and P+TA 25/75_{extracted} shows the diluting effect of triacetin. The moduli of swollen and extracted samples do differ by a factor close to $\phi_p^{1/3}$.

3) Concerning glass transition temperatures, the data of the above two (plasticized/extracted) pairs can be discusses using usual the following relationship:

$$\frac{1}{T_g} = \frac{1 - w_{TA}}{T_{gp}} + \frac{w_{TA}}{T_{gTA}} \quad (5)$$

where w_{TA} is the plasticizer mass fraction, T_{gTA} , T_{gp} and T_g are the glass transition temperatures of the plasticizer, of the polymer, and of the mixture, respectively. The data in Table 1 can be used to calculate T_{gTA} , which is the single unknown quantity. One obtains $T_{gTA} = 216$ K for the (50/50) pair and 212 K for the (25/75) pair. It can thus be considered that 214 ± 2 K is a reasonable value for the glass transition temperature of triacetin.

4) The glass transition temperatures of unplasticized networks depend of their previous history: T_{gp} is a decreasing function of the plasticizer concentration $\frac{\Delta T_{gp}}{\Delta w_{TA}} = 4$ K for the (50/50) sample and 9.3 K for the (25/75) sample, suggesting these extracted networks contain some structural irregularities that increase the polymer mobility.

5) As already addressed in the literature for similar systems [25], the comparison of the moduli for polyester-urethane P, P+TA 50/50_{extracted}, and P+TA 25/75_{extracted} suggests that the presence of a plasticizer during polymerization decreases the crosslink density.

6) According to Table 1, plasticization induces an increase of the glassy modulus. This so-called “antiplasticization” phenomenon is a very general secondary effect observed for polymers having a relatively intense β transition that is well separated from the glass transition [26,27].

7) The $\tan \delta(T)$ curve displays a single peak, showing that triacetin is fully dissolved in the polymer. The peak amplitude is an increasing function of the plasticizer content, which is not systematic in the

literature for other polymer-plasticizer mixtures (see for instance [26,28,29]). The comparison of P, P+TA 50/50_{extracted} and P+TA 25/75_{extracted} suggests this effect is not linked to the architecture of the polymer but rather to the triacetin content.

1.3. Possible initial architecture of networks

Apart from T_g changes (see Table 1), it seems that the macromolecular mobility of the networks under study can be compared through their characteristic relaxation times measured from NMR or DMA experiments. Among an impressive number of papers on NMR studies of the mobility of elastomers, examples can be found of :

- increases of relaxation times T_1 and T_2 when temperature (and mobility) increases [30],
- increases of stretched exponential relaxation times for elastomers with various crosslinking degrees at a fixed temperature [31].

Hence, T_1 and T_2 decrease when the crosslink density of the system increases [32,33], whereas they are shown to increase with the chain flexibility and mobility [33].

T_1 (longitudinal relaxation) was measured by the inversion-recovery method. The intensity of the T_1 -relaxation curve can be fitted by a sum of increasing exponential functions:

$$I = \sum_{i=1}^n A_i \cdot \left[1 - 2\exp\left(-\frac{t}{T_{1,i}}\right) \right] \quad (6)$$

where n is the number of components required to fit the relaxation curve optimally, A_i is the proportion of the i -population in the sample, and $T_{1,i}$ is the longitudinal relaxation time of the i -population. The values used for fitting the T_1 decay are given in Table 2.

	Material	P	P + TA 75/25	P + TA 50/50	P+TA 25/75	P + TA 50/50 _{extracted}	P+TA 25/75 _{extracted}
Inversion recovery	A ₁ (%)	97	90	73	49	100	100
	T _{1,1} (ms)	40	47.5	70	111	42.4	45.7
	A ₂ (%)	-	10	27	51	-	-
	T _{1,2} (ms)	-	188	208	351	-	-
Spin echo	A ₁ (%)	100	80	56	-	94	88
	T _{2,1} (ms)	0.8	0.85	1.4	-	1.1	1.5
	b	1.2	1.3	1.2	-	1.3	1.3
	A ₂ (%)	-	20	44	-	6	12
	T _{2,2} (ms)	-	44	63	-	22	27
CPMG	A ₁ (%)	80.5	46	22.5	8.1	54	51
	T _{2,1} (ms)	0.6	0.5	0.7	1.28	0.7	1.2
	b	1.2	1.5	1	1	1.5	1
	A ₂ (%)	19.5	33	30	3	37	38
	T _{2,2} (ms)	7	12	24	9	5.3	7.2
	A ₃ (%)	-	21	28	14	9	11
	T _{2,3} (ms)	-	60	107	48	17.1	40.3
	A ₄ (%)	-	-	20	26	-	-
	T _{2,4} (ms)	-	-	282	142.5	-	-
	A ₅ (%)	-	-	-	49	-	-
	T _{2,5} (ms)	-	-	-	346	-	-

Table 2. NMR longitudinal (T₁) and transversal (T₂) relaxation times.

Table 2 calls for the following comments:

- 1) For the pure polyester-urethane network, the decay of z-component of the magnetization vector can be described by a single exponential term, suggesting an homogeneous behavior at the nanometric scale.
- 2) A deviation is observed for plasticized triacetin poly(ester-urethanes) for which a second component is needed, showing a more complex behavior.
- 3) The T_{1,1} and T_{1,2} values are found to increase with triacetin ratio, which is expected to highlight an increase of mobility with triacetin for both « rigid » and « soft » phases represented by T_{1,1} and T_{1,2},

respectively. Moreover, the ratio of “soft” fraction A2 increases from 10 to 51 % when the triacetin ratio increases from 25 to 75%.

4) The relaxations of P+TA50/50_{extracted} and P+TA25/75_{extracted} can be described by the same single exponential term as the polyester-urethane polymer. They display a slight but systematic increase in T_{1,1} suggesting an increase in softness and mobility.

T₂ is a representative value of the spin-spin or transverse relaxation. The T₂ relaxation curves measured by Solid and Hahn echoes have the classical pseudo-exponential decay shape [34]. The Hahn echo sequence with varying echo time (spin echo) was deconvoluted into a sum of Lorentzian Functions using Levenberg-Marquardt algorithm. A Weibull correction was applied to the term corresponding to the shorter relaxation:

$$I = A_1 \cdot \exp\left(-\left(\frac{t}{T_{2,1}}\right)^b\right) + A_2 \cdot \exp\left(-\frac{t}{T_{2,2}}\right) \quad (7)$$

The parameters for describing the T₂ decay by spin echo are gathered in Table 2. They show that:

1) T_{2,1} and T_{2,2} increase with triacetin content by 65 and 43 %, respectively, whereas the rigid part decreases by 30%. T_{2,2} corresponds to long relaxation time processes. The corresponding component is not needed to describe the relaxation of pure polyester-urethane. It is however of increasing importance for plasticized polyester-urethane, which shows they contain segments with a higher mobility than pure polyester-urethane ones.

2) The Weibull correction is needed for all materials. Its value (b about 1.2) is quite close to the b = 1 exponent that applies to « mobile » materials (Lorentzian behavior), whereas b = 2 correspond to materials with strong dipolar coupling (Gaussian behavior).

3) The comparison of P+TA50/50 and P+TA50/50_{extracted} suggests that the behaviors of the plasticized polyester-urethanes strongly depend on the triacetin content.

4) The comparison of P+TA50/50_{extracted} and P+TA25/75_{extracted} with polyester-urethane P shows T_2 increases of 37.5 and 87.5% together with decreases in the content of rigid phase of 6 and 12%. Moreover, the comparison of P and P+TA50/50_{extracted} suggests the existence of differences in the architectures of the networks.

These results are confirmed by the T_2 values obtained by CPMG with 50 μ s between impulsions. The resulting decay curve can be fitted by the sum of Lorentzian functions:

$$I = \sum_{i=1}^n A_i \cdot \exp\left(-\frac{t}{T_{2,i}}\right) \quad (8)$$

where n is the number of components required to fit the relaxation curve optimally, A_i is the proportion of the i -population in the sample and $T_{2,i}$ the transverse relaxation time of the i -population. The A_i and $T_{2,i}$ values are gathered in Table 2 and they confirm the above observations. Triacetin seems responsible for the long relaxation modes ($T_{2,3}$ and $T_{2,4}$). Once triacetin is removed, the residual mobility of the polyester-urethane backbone seems larger when the material was synthesized in the presence of triacetin.

The samples were also tested by DMA in the frequency range 0.1-10 Hz at several temperatures. After shifting to the same reference temperature (-28°C), the tangent delta versus frequency spectra were plotted for polyester-urethane P, P+TA 50/50_{extracted} and P+TA 25/75_{extracted} (Figure 6). It is noteworthy that:

1) The higher the triacetin content for polymerization, the broader the tangent delta spectrum.

2) The networks polymerized in the presence of triacetin display a higher proportion of chain segments with low frequency relaxation. For example, tangent delta is ca. 0.6 for material P vs. 0.8 for P+TA 25/75_{extracted} at 1 Hz, and 0.05 vs. 0.35 at 0.01 Hz.

tan delta value decreases when increasing the crosslinking density of network [35] (i.e. decreasing the segmental mobility). The most reasonable explanation of the difference between tan delta spectra for polyester-urethane P on one side, and P + TA 50/50_{extracted} and P + TA 25/75_{extracted} on the other side is the existence of a population of mobile segments with a characteristic relaxation at low frequency (corresponding to high relaxation time). As it will be seen later, it seems in full agreement with the possible existence of dangling chains and loops in polyester-urethane P+TA 50/50_{extracted} and P+TA 25/75_{extracted}, the proportion of which increases with the concentration in triacetin used during the polymerization of networks.

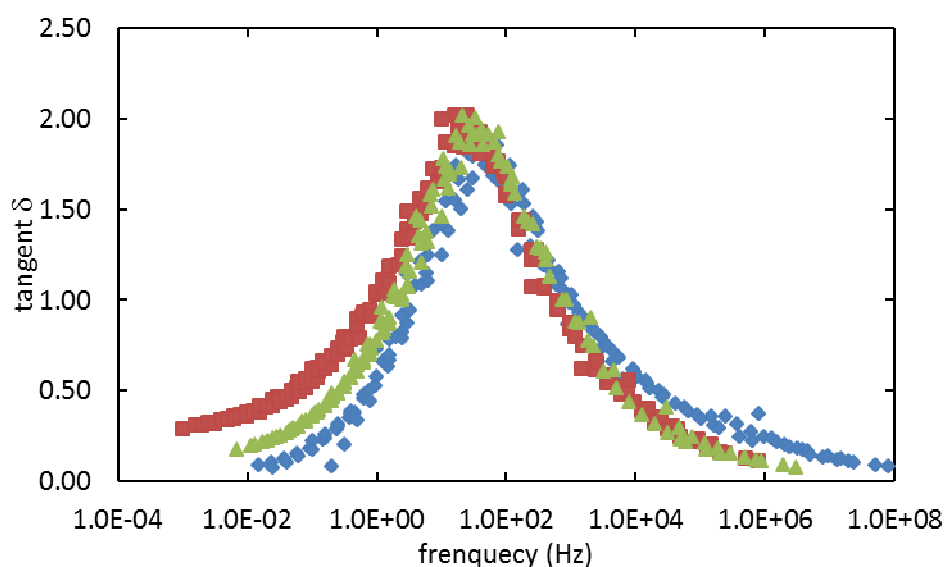


Figure 6. Tangent delta spectra for polyester-urethane P (◆), P+TA 50/50_{extracted} (▲) and P+TA 25/75_{extracted} (■) at -28°C.

Dangling chains can alternatively be characterized by their effects on relaxation properties. The relaxation modulus can be described by a relation proposed by Chasset and Thirion [36]:

$$E = E_{\infty} \cdot [1 - (t/\tau_0)^{-m}] \quad (9)$$

The analysis of several EPDMs showed a strong increase of τ_0 when the crosslinking level decreased and when the dangling chain content increased [37]. Comparable results were found for PDMS differing by the number and the length of dangling chains [38]. The exponent m is also shown to increase [36], despite being expected independent of the concentration of dangling chains [38]. According to McKenna [39], m is a material parameter which is independent of the crosslink density but which is temperature dependent. The P, P+TA 50/50_{extracted} and P+TA 25/75_{extracted} networks cannot be considered as “iso state” at a given temperature. Hence, we only focused on τ_0 : this parameter increases for polymers cured in the presence of triacetin, consistently with the longer relaxation process of dangling chains (Table 3).

	P	P + TA 50/50 _{extracted}	P + TA 25/75 _{extracted}
τ_0 (ms)	0.614-6.2	11.9-15.9	44-65.3

Table 3. Characteristic relaxation times of extracted polyester-urethanes.

2. Ageing results

Hydrolysis leads to the cleavage of ester groups. If the latter belong to elastically active chains, this induces a decrease of the elastic modulus and an increase of the swelling ratio. The changes of these two macroscopic properties were used for estimating the depletion in [EAC] (Figure 7). The hydrolysis rate was derived from Figure 7 by:

$$d[\text{EAC}]/dt = -r \quad (10)$$

The evolutions of the hydrolysis rates with the triacetin content for networks polymerized in the presence of triacetin are shown in Table 4. The degradation rate is a decreasing function of the percentage of triacetin, at least when the latter is added to the polymer during its polymerization process.

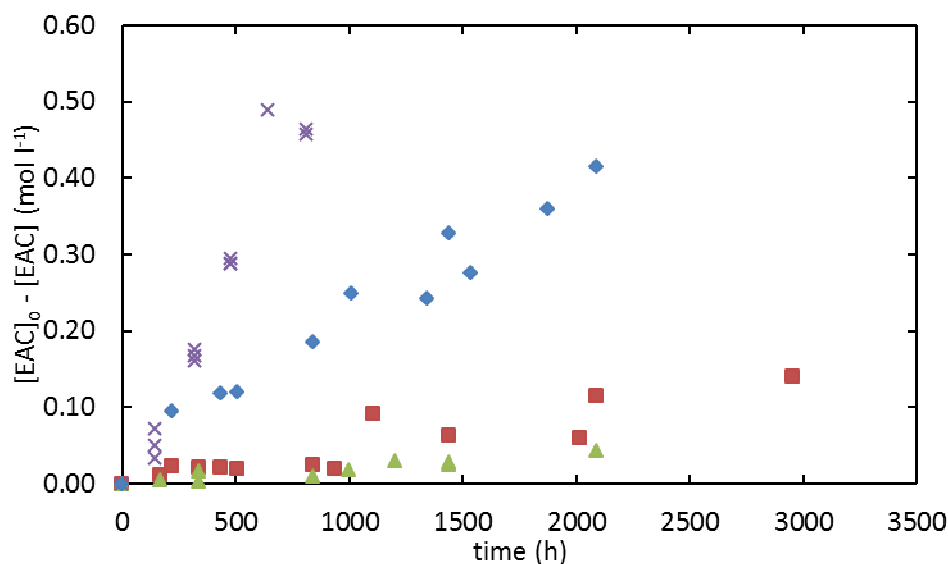


Figure 7. Changes in the concentration of elastically active chains after ageing at 60°C under 75%RH for polyester-urethane P (x), P+TA 75/25 (◆), P+TA 50/50 (■), P+TA 25/75 (▲).

	pure	75/25	50/50	25/75
75%HR*	482	202	44	36.5
75%HR**	597	356	26	50.3
29%HR**	96.4	78.2		8

Table 4. Rate of elastically active chains loss ($10^{-6} \text{ mol l}^{-1} \text{ s}^{-1}$) from swelling (*) or from mechanical properties (**) at 60°C.

DISCUSSION

The aim of this section is to establish a link between the two main results of this paper: (i) the presence of triacetin during synthesis induces some defects in the network architecture, and (ii)

networks polymerized in the presence of triacetin are less sensitive to hydrolytic degradation. Let us first recall that:

1) For any kind of ester:

$$d[E]/dt = -k_H \cdot [H_2O][E] \quad (11)$$

2) For esters hold by elastically active chains:

$$d[E]_{EAC}/dt = ds/dt = -k_H \cdot [H_2O][E]_{EAC} \quad (12)$$

3) For ideal networks at low conversion degrees:

$$d[EAC]/dt = -\psi \cdot ds/dt \quad (13)$$

where $\psi = 3$ in a trifunctional network, $\psi = 1$ in a network of higher functionality [40], ds/dt is the rate of ester hydrolysis, $[E]_{EAC}$ and $[E]$ are the concentration in esters hold by the elastically active chains and the overall ester concentration, respectively. Therefore:

$$d[EAC]/dt = -\psi \cdot k_H \cdot [E]_{EAC}[H_2O] \quad (14)$$

The trends summarized in Table 4 will hence be discussed regarding the parameters ψ , k_H , $[H_2O]$ and $[E]_{EAC}$, which govern the rate of degradation. First, according to Figure 3, the difference in hydrophilicity (i.e., the $[H_2O]$ term in Eq. 14) does not seem to be a sufficient explanation and will not be discussed further in the following. The results in Table 4 can thus be discussed considering a change in the apparent rate constant for hydrolysis reaction k_H and a change in the network architecture modifying $[E]_{EAC}$ or the ψ parameter.

1. On the hydrolytic stability of triacetin

Triacetin hydrolysis would generate acetic acid, which is a powerful catalyst of network hydrolysis [15] and would complexify the mathematical treatment of our results [8]. In order to analyze the hydrolytic stability of triacetin within the timescale investigated, it was exposed directly to 75%RH at 60°C. The changes in the triacetin structure were monitored by FTIR, which gives the concentration of unreacted esters. The spectra of virgin and aged (up to 1992 h) triacetins are presented in Figure

8. The pristine triacetin displays a maximal absorbance at 1735 cm^{-1} ascribed to the ester group. During exposure, the intensity of this band decreases and the band becomes broader because esters are converted into carboxylic acids absorbing at ca. 1710 cm^{-1} . The quantitative analysis is complicated because FTIR spectra of these two groups overlap partially. Moreover, since the triacetin molecule holds 3 esters, the overall ester depletion does not give the concentration in unreacted triacetin. HPLC complementary experiments were hence performed (see Appendix) and showed that triacetin can be considered as almost stable in a first approach.

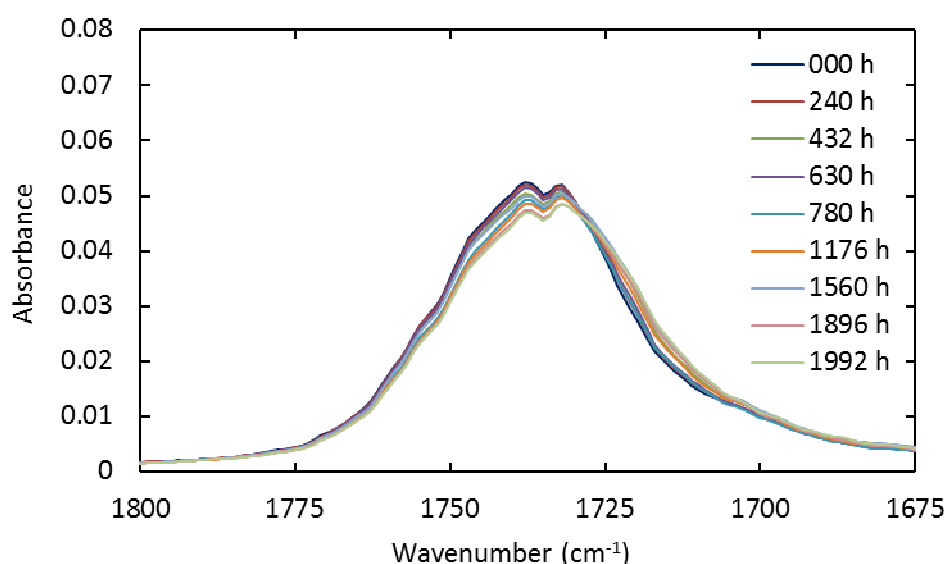


Figure 8. FTIR spectra of triacetin after several durations of exposure to 75%RH at 60°C.

2. On the effect of triacetin on the hydrolysis rate

Some comparisons were done with materials differing by:

- 1) the presence of triacetin, i.e., a comparison of polyester-urethanes in which triacetin was extracted or not prior to ageing (see 'EXPERIMENTAL'),
- 2) the method for adding triacetin, i.e., during or after polymerization, to investigate if a slower hydrolysis kinetics is due to the presence of triacetin or to a difference in the polymer architecture.

The hydrolysis kinetics of polyester-urethanes in which triacetin was removed (P+TA 50/50_{extracted}, P+TA 25/75_{extracted}) or not (P+TA 50/50, P+TA 25/75) prior to ageing is presented in Figure 9. It appears that hydrolysis develops faster in purified polyester-urethanes P+TA 50/50_{extracted} and P+TA 25/75_{extracted} than in plasticized ones P+TA 50/50 and P+TA 25/75. If triacetin is hydrolytically stable within the timescale investigated, the rate of hydrolysis in plasticized polyester-urethane r_{P+TA} can be expressed as:

$$r_{P+TA} = k_H[H_2O][E]_{EAC} \cdot \phi_P \quad (15)$$

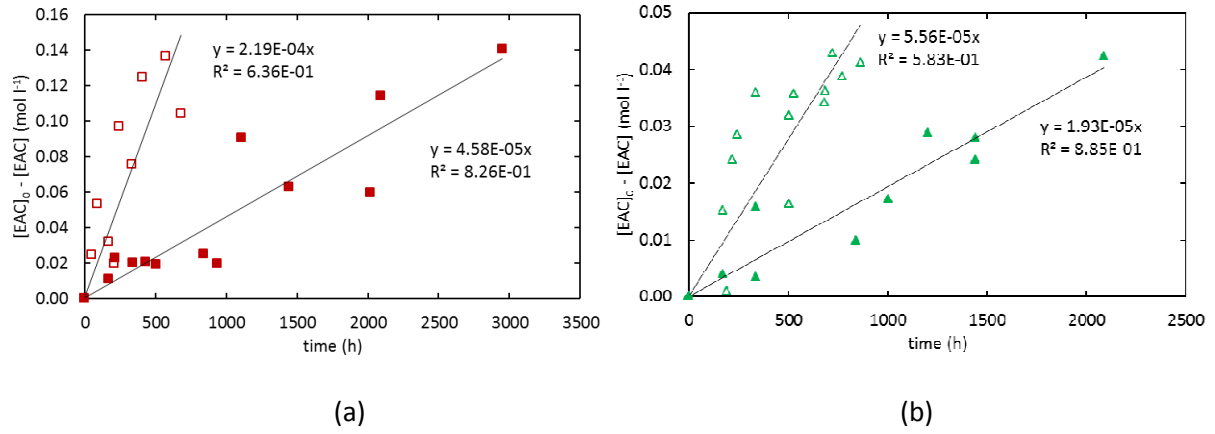


Figure 9. Changes in elastically active chains concentration at 60°C and 75% RH for polyester-urethanes (a) P+TA 50/50 (■) and P+TA 50/50_{extracted} (□), (b) P+TA 25/75 (▲) and P+TA 25/75_{extracted} (△).

where $[E]_{EAC}$ is the concentration in esters held by elastically active chains in the unplasticized polymer and ϕ_P is the polymer volume ratio (almost equal to its weight fraction). Therefore:

$$r_{P+TA} = k_H[H_2O][E]_{EAC} \cdot (1 - w_{TA}) \quad (16)$$

where w_{TA} is the volume fraction of triacetin. If r_P is the rate of hydrolysis in pure polyester-urethane:

$$r_{P+TA} = r_P \cdot (1 - w_{TA}) \quad (17)$$

Another reasoning taking into account the triacetin reactivity can also be proposed (see APPENDIX B), and the two hypotheses lead to the same conclusion that the hydrolysis rate of elastically active chains should decrease when the triacetin weight ratio increases.

This triacetin effect was studied by comparing the degradation rates of polyester-urethanes in which triacetin was added either directly during polymerization (P+TA 75/25 and P+TA 50/50) or after polymerization (P+TA 75/25_{impregnated} and P+TA 50/50_{impregnated}). If triacetin would have only a diluting effect on the reactive ester groups, the rate of hydrolysis in P+TA 75/25 (respectively P+TA 50/50) would be the same as in P+TA 75/25_{impregnated} (respectively P+TA 50/50_{impregnated}). This assessment is rather well verified for the polyester-urethane P+TA 75/25 but, according to Figure 10, a significant change is observed for the P+TA 50/50 network, indicating that the impregnated network undergoes a faster hydrolysis. Given their similar triacetin contents and hydrophilicities (Figure 3), the difference between P+TA 50/50 and P+TA 50/50_{impregnated} is their initial architecture (proportions of elastically active chains, dangling chains, loops, etc.), so that an intrinsic difference in their sensitivities to hydrolysis expressed by either ψ or $[E]_{EAC}$ in Eq. 4 and 5 must apply.

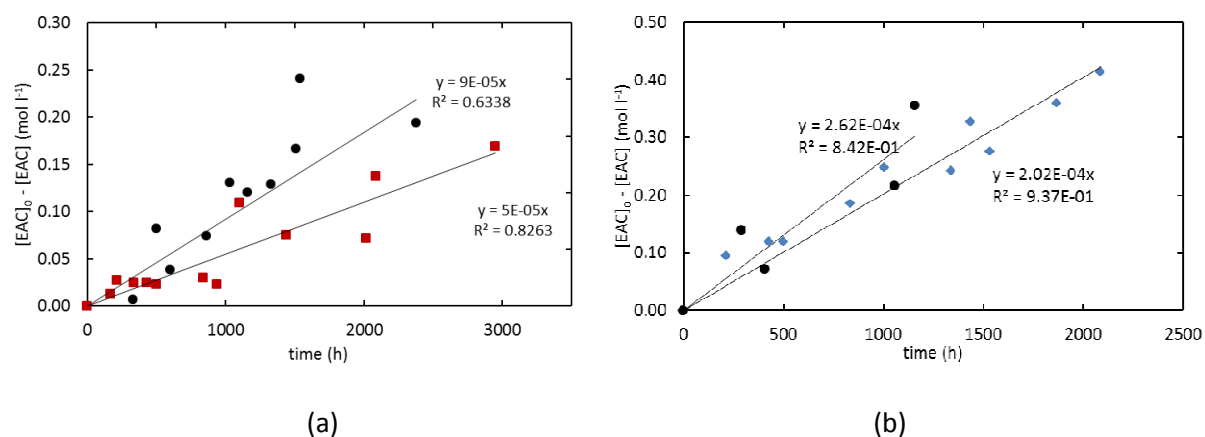


Figure 10. Changes in elastically active chains concentration at 60°C and 75% RH for polyester-urethanes (a) P+TA 50/50(■) and P+TA 50/50_{impregnated} (●), (b) P+TA 75/25 (◆) and P+TA 75/25_{impregnated} (●).

This analysis could not be applied to 25/75 mixtures because it was not possible to reach such a high ratio by impregnating a polyester-urethane with triacetin (Figure 2). Under the assumption that the limit solubility of triacetin in polyester-urethane depends mainly on the crosslinking density, this confirms that the architecture of “pure” polyester-urethane and of polyester-urethane polymerized in the presence of 75% of triacetin are significantly different (see Table 1).

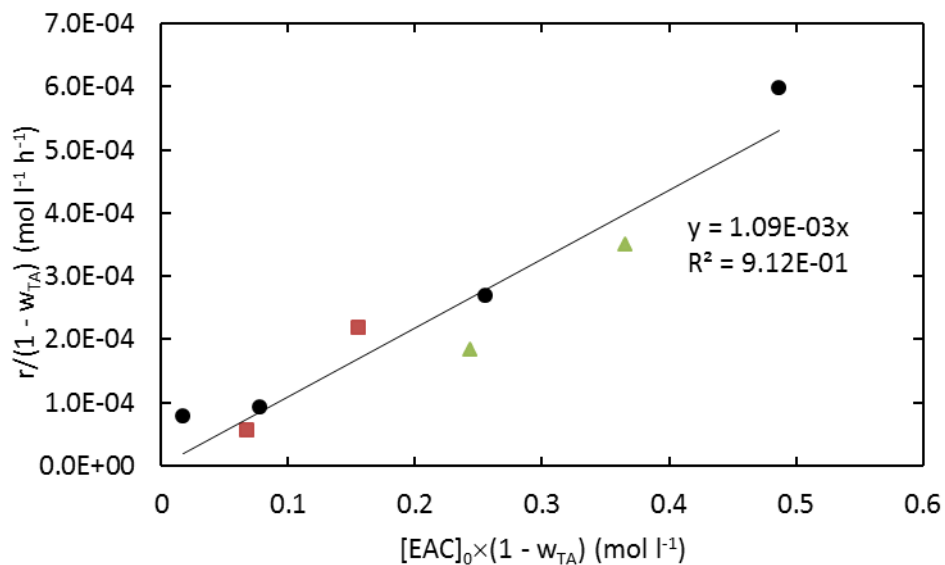


Figure 11. Rate of network degradation as a function of elastically active chains (●: P + TA, ■: P + TA_{impregnated}, ▲: P + TA_{extracted}).

The overall results can be discussed by plotting the rate at which EACs are actually degraded $r/(1 - w_{TA})$ vs. the actual elastically active chains concentration in plasticized polymer $[EAC]_0 \times (1 - w_{TA})$. Figure 11 confirms that triacetin plays a diluting role first, but there remains to explain the dependency of $[EAC]_0$ on the triacetin concentration in the polymerization medium.

3. On the presence on loops in networks

The most reasonable explanation of the above dependency comes from theories first proposed by Jacobson and Stockmayer [41] and later illustrated by Stepto [42], Dušek et al. [43] and Elliot et al. [44], about the effect of the dilution of the reactive medium during polymerization on the final network architecture. According to these theories, the higher the ratio of triacetin added to polyester-urethane at the polymerization step, the higher the probability to get loops, the hydrolytic degradation of which has a negligible effect on the polymer elastic properties.

Let us consider four distinct and very simple gel structures (Figure 12) differing by their molar mass between crosslinks (and tentatively representing the networks P, P+TA 50/50_{extracted} and P+TA

25/75_{extracted} characterized in Table 1). These representations are considered here as heuristics since real structures are no doubt much more complex. Schematically:

1) Case 1 corresponds to polyester-urethane P ($M_c \sim 2 \text{ kg mol}^{-1}$ corresponding to a $E'_{\text{rubbery}} = 4.4 \text{ MPa}$ instead of an experimental value of 3.6).

2) Case 2 corresponds to polyester-urethane with $M_c \sim 8 \text{ kg mol}^{-1}$ (corresponding to a $E'_{\text{rubbery}} = 1.1 \text{ MPa}$ instead of an experimental value of 0.9). It is here assumed that P+TA 50/50_{extracted} behaves like a mixture of network 1 + network 2 with 1:2 mass ratios.

3) Cases 3 and 4 correspond to polyester-urethanes with $M_c \sim 14 \text{ kg mol}^{-1}$ (corresponding to a $E'_{\text{rubbery}} = 0.6 \text{ MPa}$ instead of an experimental value of 0.5) not too far from the P+TA 25/75_{extracted} value.

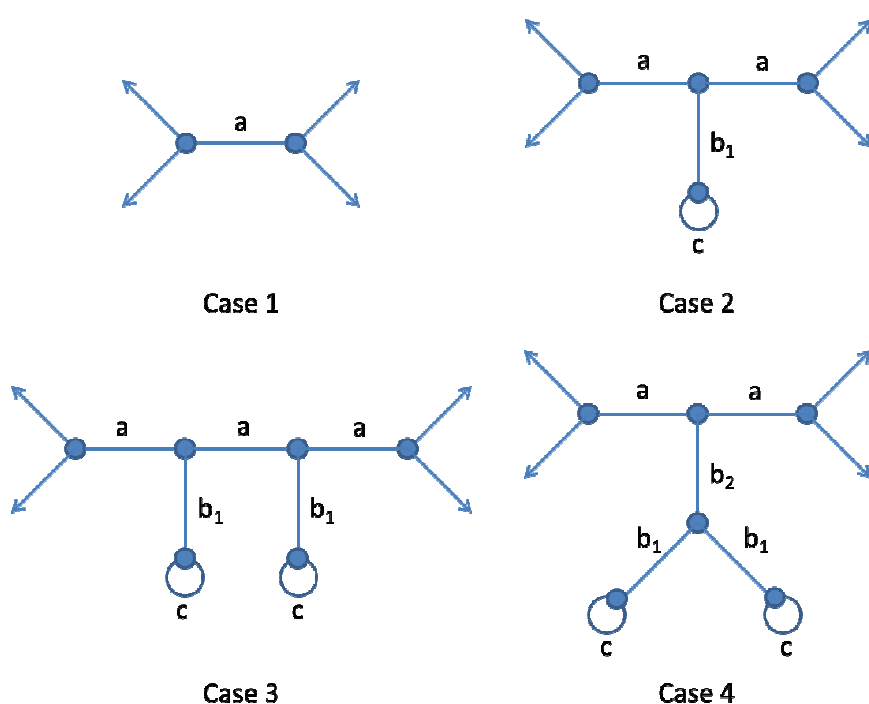


Figure 12. Simple representations of networks with various molar masses between crosslinks.

Under the assumption that ester hydrolysis is a random process and can occur on elastically active chains, dangling chains, or terminal loops, it can be concluded that for low conversion degrees:

- 1) Scission of an EAC of “a” type leads to the disappearance of 3 EACs but no increase of the sol.
- 2) Scission of a “b₁” chain does not change the EAC number, meanwhile 1.5 chain is converted into soluble material (NB: 1.5 means that “b₁” chains are more or less cut in their middle, on average).

- 3) Scission of a “b₂” chain does not change the EAC number, meanwhile 4.5 chains are converted into soluble material.
- 4) Scission of a “c” chain does not change either EAC or soluble fraction.

It seems clear that the yield of soluble fraction per EAC consumption increases for materials with a larger proportion of dangling chains and loops (Table 5), which is expected for samples polymerized in the presence of triacetin. Because the “model” networks are very crude approximations (Figure 12) and because of the data scattering (Figure 13), the above reasoning is more a rough justification of the observed trend than a quantitative prediction of the experimental values. However, it seems in accordance with the data in Figure 13, which shows the soluble fraction change per hydrolysis event expressed by the elastically active chains relative decrease $([EAC]_0 - [EAC])/[EAC]_0$ (instead of $\Delta[EAC]$ in Table 5, which is a “number of elastically active chains lost”).

Case	Chain	probability	$\Delta[EAC]$	ΔFS	$\Delta FS/\Delta[EAC]$
1	a	1	3	0	0
2	a	1/2	3	0	1/4
	b ₁	1/4	0	1.5	
	c	1/4	0	0	
3	a	3/7	3	0	1/3
	b ₁	2/7	0	1.5	
	c	2/7	0	0	
4	a	2/7	3	0	5/4
	b ₁	2/7	0	1.5	
	b ₂	1/7	0	4.5	
	c	2/7	0	0	

Table 5. Impacts of chain scissions on the elastically active chains concentration ($[EAC]$) and on the soluble fraction (SF) for the networks schematized in Figure 12.

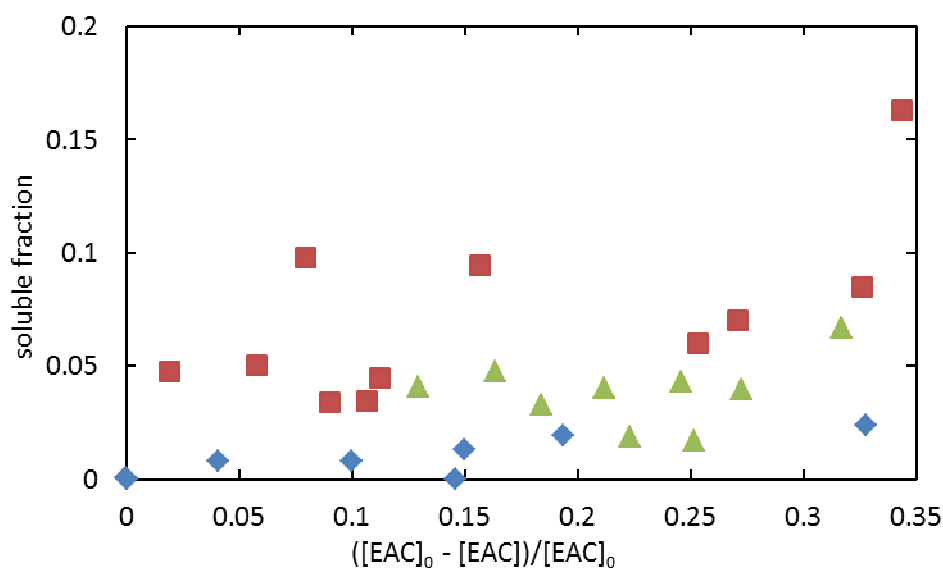


Figure 13. Soluble fraction vs. relative decrease of elastically active chains concentration for polyester-urethane P (◆), P+TA 50/50_{extracted} (▲) and P+TA 25/75_{extracted} (■).

CONCLUSIONS

This paper compared the hydrolytic stability of fully cured polyester-urethanes polymerized in the presence of triacetin. It was shown that the presence of triacetin does not change the polymer affinity with water. Hydrolytic degradation rate (judged from the crosslink density decrease) at early stages was shown to decrease when the triacetin content increased, at least when the latter is added directly in the polymerization medium. Comparisons of the hydrolysis of networks in which triacetin was introduced either during or after polymerization pointed out that the polymer synthesized in the presence of triacetin is less sensitive to hydrolytic degradation because of the existence of inelastic chains whose hydrolysis does not induce a change of elastic modulus or equilibrium swelling ratio. This hypothesis was confirmed by measurements of NMR and DMA relaxation times.

ACKNOWLEDGEMENTS

The Direction Générale de l'Armement is acknowledged for the funding of this work.

APPENDIX A: STABILITY OF TRIACETIN STUDIED BY HPLC

The hydrolytic stability of triacetin was checked by HPLC analysis of aged triacetin using a Waters 717+ apparatus with C18 Column as stationary phase and acetonitrile (0.3 ml min^{-1}) as mobile phase. Mobile phase was detected using UV detection at 210 nm at which triacetin displays a maximal absorbance. Column and UV detector temperatures were maintained respectively at 40 and 35°C. The calibration made on several samples with concentrations ranging from 0 to 110 g l^{-1} lead to the following relationship:

$$\text{Abs(TA 210nm)} = 1.463 \cdot 10^{-4} \cdot [\text{TA}] \quad (R^2 = 0.996) \quad (18)$$

Figure 14 displays the changes of unreacted triacetin content during 60°C 75%RH exposure and confirms FTIR observations according to which TA is stable within the investigated timescale.

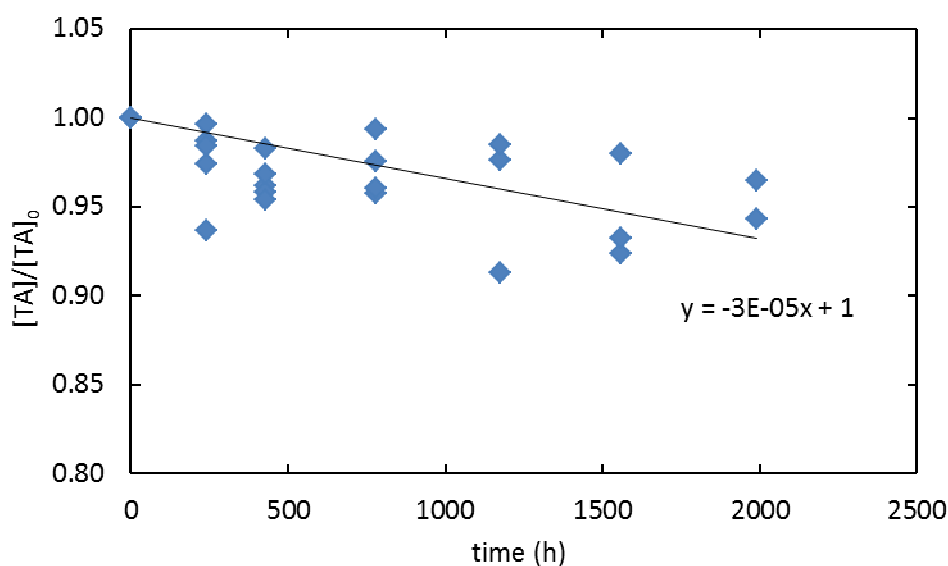


Figure 14. Residual triacetin content estimated from HPLC measurements after exposure at 60°C under 75% RH.

APPENDIX B: ON THE DILUTING EFFECT OF TRIACETIN ON HYDROLYSIS RATE

If triacetin is hydrolysable, the rate of hydrolysis of ester in polyester-urethane r_p and in triacetin r_{TA} can be expressed as:

$$r_p = k_p[H_2O][E_p] \quad (19)$$

$$r_{TA} = k_{TA}[H_2O][E_{TA}] \quad (20)$$

where E_p and E_{TA} are the concentrations of esters hold by polyester-urethane and by triacetin, respectively. Since esterified adipic acid (AA) and triacetin hold 2 and 3 esters per monomer unit/molecule, respectively:

$$r_p = 2k_p[H_2O][AA] \quad (21)$$

$$r_{TA} = 3k_{TA}[H_2O][TA] \quad (22)$$

where $[AA]$ is the concentration of adipate monomer units. The ratio of EAC decrease in polyester-urethane + triacetin compared to the purified polyester-urethane is thus given at low conversion degrees by:

$$\frac{r_p}{r_p + r_{TA}} = \frac{2k_p[AA]}{2k_p[AA] + 3k_{TA}[TA]} \quad (23)$$

Which can be simplified by supposing in a first approach that triacetin esters are less reactive than polyester-urethane ($k_{TA} \ll k_p$) to give:

$$\frac{r_p}{r_p + r_{TA}} = \frac{1}{1 + \frac{3k_{TA}w_{TA}M_{AA}}{2k_{AA}w_{AA}M_{TA}}} \sim 1 - \frac{3k_{TA}w_{TA}M_{AA}}{2k_{AA}(1-w_{TA})M_{TA}} \quad (24)$$

Eq 24 illustrates the “diluting” effect of triacetin leading to a decrease of hydrolysis rate.

REFERENCES

1. T.S. Ellis, F.E. Karasz. Interaction of epoxy resins with water: the depression of glass transition temperature. *Polymer* 1984;25(5):664-669.
2. A. Apicella, C. Migliaresi, L. Nicolais, L. Iaccarino, S. Roccotelli. The water ageing of unsaturated polyester-based composites: influence of resin chemical structure. *Composites* 1983;14(4):387-392.
3. M. Partini, R. Pantani. FTIR analysis of hydrolysis in aliphatic polyesters. *Polym Degrad Stab* 2007;92(8):1491-1497.
4. F. Bélan, V. Bellenger, B. Mortaigne, J. Verdu, Y.S. Yang. Hydrolytic stability of unsaturated polyester prepolymers. *Compos Sci Tech* 1996;56(7):733-737.
5. K.A. Barrera-Rivera, L. Peponi, Á. Marcos-Fernández, J.M. Kenny, A. Martínez-Richa. Synthesis, characterization and hydrolytic degradation of polyester-urethanes obtained by lipase biocatalysis. *Polym Degrad Stab* 2014;108:188-194.
6. F. Bélan, V. Bellenger, B. Mortaigne, J. Verdu. Relationship between the structure and hydrolysis rate of unsaturated polyester prepolymers. *Polym Degrad Stab* 1997;56(3):301-309.
7. B. Jacques, M. Werth, I. Merdas, F. ThomINETTE, J. Verdu. Hydrolytic ageing of polyamide 11. 1. Hydrolysis kinetics in water. *Polymer* 2002;43(24):6439-6447.
8. L.J. Kasehagen, I. Haury, C.W. Macosko, D.A. Shimp. Hydrolysis and blistering of cyanate ester networks. *J Appl Polym Sci* 1997;64(1):107-113.
9. E. Richaud, P. Gilormini, M. Coquillat, J. Verdu. Crosslink Density Changes during the Hydrolysis of Tridimensional Polyesters. *Macromol Theor Simul* 2014;23(5):320–330.
10. Y. Ren, S. Zhao, Q. Li, X. Zhang, L. Zhang. Influence of liquid isoprene on rheological behavior and mechanical properties of polyisoprene rubber. *J Appl Polym Sci* 2015;132(8) DOI: 10.1002/app.41485.
11. Z. Wang, Y. Han, Z. Huang, X. Zhang, L. Zhang, Y. Lu, T. Tan. Plasticization effect of hydrogenated transgenic soybean oil on nitrile-butadiene rubber. *J Appl Polym Sci* 2014;131(16). DOI: 10.1002/app.40643.
12. G.A. Yilmaz, D. Şen, Z.T. Kaya, T. Tinçer. Effect of inert plasticizers on mechanical, thermal, and sensitivity properties of polyurethane-based plastic bonded explosives. *J Appl Polym Sci* 2014;131(20). DOI: 10.1002/app.40907.
13. J. Jeczalik. Action of hydrocarbon and ester plasticizer in urethane elastomer for sealing purposes. *J Appl Polym Sci* 2011;81(3):523-529.
14. J.D. Badia, T. Kittikorn, E. Strömberg, L. Santonja-Blasco, A. Martínez-Felipe, A. Ribes-Greus, M. Ek, S. Karlsson. Water absorption and hydrothermal performance of PHBV/sisal biocomposites. *Polym Degrad Stab* 2014;108:166–174.
15. S. M. Martelli, G. Moore, S. Silva Paes, C. Gandolfo, J. Borges Laurindo. Influence of plasticizers on the water sorption isotherms and water vapor permeability of chicken feather keratin films. *LWT - Food Sci Technol* 2006;39(3):292-301.
16. S. Hocker, A.K. Rhudy, G. Ginsburg, D.E. Kranbuehl. Polyamide hydrolysis accelerated by small weak organic acids. *Polymer* 2014;55(20):5057-5064.

-
17. E. Raphaël, C. Gay, P.G. de Gennes. Progressive Construction of an "Olympic" Gel. *J Stat Phys* 1997;89(1/2):111-118.
 18. Z.S. Petrović, M. Ionescu, J. Milć, J.R. Halladay. Soybean oil plasticizers as replacements of petroleum oil in rubber. *Rubber Chem Technol* 2013;86(2):233–249.
 19. Y. Ren, S. Zhao, Q. Li, X. Zhang, L. Zhang. Influence of liquid isoprene on rheological behavior and mechanical properties of polyisoprene rubber. *J Appl Polym Sci* 2015;132(8). DOI: 10.1002/app.41485.
 20. J.E. Mark, A. Eisenberg, W.W. Graessley, L. Mandelkern, J.L. Koenig. *Physical Properties of Polymers*, Washington DC, ACS, 1984, pp. 1-54.
 21. G.C. Borgia, P. Fantazzini, A. Ferrando, G. Maddinelli. Characterisation of crosslinked elastomeric materials by ¹H NMR relaxation time distributions. *Magn Reson Imaging* 2001;19(3–4):405-409.
 22. S. Hayashi, Y. Komori. Determination of residual dipolar interaction from transverse ¹H NMR relaxation in elastomers. *Solid State Nucl Mag* 2009;36(4):167-171.
 23. E. Fukushima, S.B. Roeder. in "Experimental Pulse NMR : A Nuts and Bolts Approach" (1996), Addison-Wesley Publishing Company.
 24. Flory P.J. *Principles of polymer chemistry*. Ithaca, NY: Cornell University Press; 1953.
 25. A. Azoug, R. Nevière, R.-M. Pradeilles-Duval, A. Constantinescu. Influence of crosslinking and plasticizing on the viscoelasticity of highly filled elastomers. *J Appl Polym Sci* 2014;131(12). DOI: 10.1002/app.40392.
 26. N. Kinjo, T. Nakagawa. Antiplasticization of Slightly Plasticized Poly(vinyl chloride). *Polym J* 1973;4(2):143-153.
 27. L.M. Robeson, J.A. Faucher. Secondary loss transitions in antiplasticized polymers. *Polym Letters* 1969;7:35-40.
 28. R. Thomas, S. Durix, C. Sinturel, T. Omonov, S. Goossens, G. Groeninckx, P. Moldenaers, S. Thomas. Cure kinetics, morphology and miscibility of modified DGEBA-based epoxy resin – Effects of a liquid rubber inclusion. *Polymer* 2007;48(6):1695-1710.
 29. G.G. Liang, W.D. Cook, A. Tcharkhtchi, H. Sautereau. Epoxy as a reactive plasticizer for improving polycarbonate processibility. *Eur Polym J* 2011 ;47(8):1578-1588.
 30. P.P. Sukhanov, V.S. Minkin, V.I. Kimel'blat. Study of branched oligoesters and crosslinked polyurethane elastomer by the NMR method. *Polymer Science U.S.S.R.*, Volume 25, Issue 2, 1983, Pages 264-274.
 31. L. Gasper, D.E. Demco, B. Blümich. Proton residual dipolar couplings by NMR magnetization exchange in cross-linked elastomers: determination and imaging. *Solid State Nuclear Magnetic Resonance*, Volume 14, Issue 2, July 1999, Pages 105-116.
 32. A. Azoug, A. Constantinescu, R. Nevière, G. Jacob. Microstructure and deformation mechanisms of a solid propellant using ¹H NMR spectroscopy. *Fuel*, Volume 148, 15 May 2015, Pages 39-47.
 33. N. Ducruet, L. Delmotte, G. Schrodj, F. Stankiewicz, N. Desgardin, M.-F. Vallat, B. Haidar Evaluation of hydroxyl terminated polybutadiene-isophorone diisocyanate gel formation during crosslinking process. *Journal of Applied Polymer Science*, Volume 128, Issue 1, 5 April 2013, Pages: 436–443.
 34. D.E. Demco, A.-M. Oros-Peusquens, L. Utu, R. Fechete, B. Blümich, N. Jon Shah. Molecular dynamics parameter maps by ¹H Hahn echo and mixed-echo phase-encoding MRI. *J Magn Reson* 2013;227:1-8.

-
35. J. Davenas, I. Stevenson, N. Celette, G. Vigier, L. David. Influence of the molecular modifications on the properties of EPDM elastomers under irradiation. *Nucl Instrum Meth B* 2003;208:461-465.
36. Chasset R, Thirion P. In: Prins JA, editor. Proceedings of the conference on physics of non-crystalline solids. Amsterdam: North Holland; 1965. p. 345.
37. G. Martin, C. Barrès, P. Cassagnau, P. Sonntag, N. Garois. Viscoelasticity of randomly crosslinked EPDM networks. *Polymer* 2008 ;49(7):1892-1901.
38. L.E. Roth, D.A. Vega, E.M. Vallés, M.A. Villar. Viscoelastic properties of networks with low concentration of pendant chains. *Polymer* 2004;45(17):5923-5931.
39. G.B. McKenna, R.J. Gaylord. Relaxation of crosslinked networks: theoretical models and apparent power law behaviour. *Polymer* 1988;29(11):2027-2032.
40. J. Verdu. Structural Changes Caused by Oxidation. In: *Oxidative Ageing of Polymers*. Chapitre 7. Pages: 163–201 (2013). Published Online : 21 JAN 2013, DOI: 10.1002/9781118562598.ch7
41. H. Jacobson, W.H. Stockmayer. Intramolecular reaction in polycondensations. I. The theory of linear systems. *J Chem Phys* 1950;18(12):1600-1606.
42. S. Dutton, R.F.T. Stepto, D.J.R. Taylor. Formation, structure and properties of polymer networks. *Macromolecular Symposia* 1997;118(1):199–205.
43. M. Dušková-Smrčková, H. Valentová, A. Ďuračková, K. Dušek. Effect of Dilution on Structure and Properties of Polyurethane Networks. Pregel and Postgel Cyclization and Phase Separation. *Macromolecules* 2010;43(15):6450–6462.
44. J.E. Elliott, M. Macdonald, J. Nie, C.N. Bowman. Structure and swelling of poly(acrylic acid) hydrogels: effect of pH, ionic strength, and dilution on the crosslinked polymer structure. *Polymer* 2004;45(5):1503-1510.